

Identification of Ligands for the Tau Exon 10 Splicing Regulatory Element RNA by Using Dynamic Combinatorial Chemistry

Paula López-Senín,^[a] Irene Gómez-Pinto,^[b] Anna Grandas,^[a] and Vicente Marchán*^[a]

Abstract: We describe the use of dynamic combinatorial chemistry (DCC) to identify ligands for the stem-loop structure located at the exon 10-5'-intron junction of Tau pre-mRNA, which is involved in the onset of several tauopathies including frontotemporal dementia with Parkinsonism linked to chromosome 17 (FTDP-17). A series of ligands that combine the small aminoglycoside neamine and heteroaromatic moieties (azaquinolone and two acridines) have been identified by using

DCC. These compounds effectively bind the stem-loop RNA target (the concentration required for 50% RNA response (EC_{50}): 2–58 μM), as determined by fluorescence titration experiments. Importantly, most of them are able to stabilize both the wild-type and

Keywords: combinatorial chemistry • molecular recognition • RNA ligands • RNA structures • template synthesis

the +3 and +14 mutated sequences associated with the development of FTDP-17 without producing a significant change in the overall structure of the RNA (as analyzed by circular dichroism (CD) spectroscopy), which is a key factor for recognition by the splicing regulatory machinery. A good correlation has been found between the affinity of the ligands for the target and their ability to stabilize the RNA secondary structure.

Introduction

RNA plays an essential role in many cellular processes, from the regulation of gene expression to protein synthesis, as well as in the progression of viral diseases. This macromolecule is able to adopt more complex three-dimensional structures than those of DNA; they are similar to those observed in proteins, and the tertiary structure is, as yet, difficult to predict. Hence, the discovery of selective and, more importantly, specific ligands for this macromolecule represents a challenge for medicinal and bioorganic chemistry and therapy.^[1] However, most of the known RNA-binding ligands can each bind to several different RNA targets of unrelated sequence and structure,^[2] which compromises their biological application. We hypothesize that higher af-

finity and better specificity could be achieved by combining two or more small molecules with different affinities and abilities to recognize some of the secondary structural motifs present in a particular RNA target.^[3] This fragment-based lead-discovery search approach,^[4] in combination with dynamic combinatorial chemistry (DCC),^[5] offers new perspectives and opportunities for identifying RNA ligands, as well as for improving our understanding of RNA recognition mechanisms.

Over the past few years, DCC has demonstrated its potential as a tool for the discovery of ligands for biomolecules, mainly because both the library synthesis and the affinity screening steps are carried out simultaneously in a single process.^[5] In the field of nucleic acids, DCC has been used to select a copper(II) coordination complex that binds to an RNA hairpin,^[6] as well as ligands that bind to DNA duplex or quadruplex structures,^[7] and also to stabilize oligonucleotide complexes by covalent linkage of small molecules.^[8] More recently, resin-bound DCC has been used to identify ligands for RNA structures involved in HIV-1 replication and in myotonic dystrophy type 1.^[9] Typically, most ligands for DNA and RNA targets that have been identified by using DCC have high-to-medium affinities ($\approx 2\text{--}50\ \mu\text{M}$).

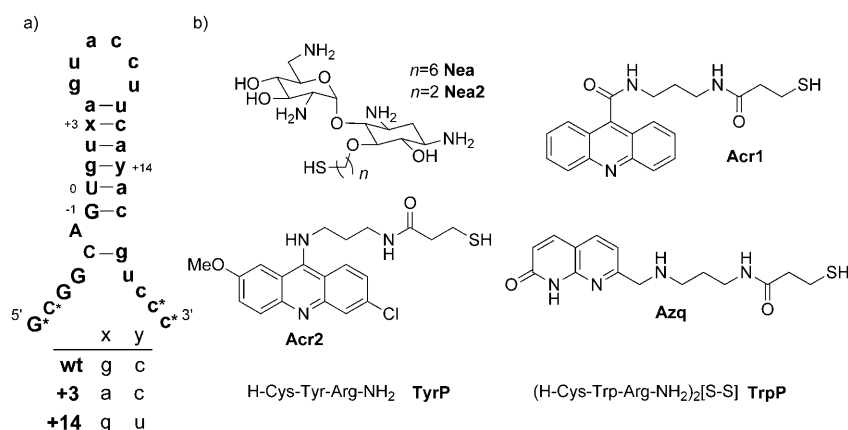
In the study reported here, we use DCC to identify ligands for the Tau exon 10 splicing regulatory element RNA involved in frontotemporal dementia with parkinsonism

[a] P. López-Senín, Prof. A. Grandas, Dr. V. Marchán
Departament de Química Orgànica and IBUB
Universitat de Barcelona, Martí i Franquès 1-11
08028 Barcelona (Spain)
Fax: (+34)93-339-7878
E-mail: vmarchan@ub.edu

[b] Dr. I. Gómez-Pinto
Instituto de Química-Física Rocasolano
CSIC, Serrano 119, 28006 Madrid (Spain)

Supporting information for this article is available on the WWW under <http://dx.doi.org/10.1002/chem.201002065>.

linked to chromosome 17 (FTDP-17).^[10] Tau is a microtubule-associated protein that is required for the polymerization and stability of microtubules, as well as for axonal transport in neurons. In a normal adult human brain, alternative splicing of exons 2, 3, and 10 produces six tau isoforms with either three (3R) or four (4R) repeat domains, with a 4R/3R ratio of approximately 1.^[11] However, mutations found in the tau gene of FTDP-17 patients, especially at the exon 10-5'-intron junction, alter pre-mRNA splicing and result in an increase in the inclusion of exon 10. The normal one-to-one isoform balance is thus perturbed, with the 4R isoform being overproduced in most cases. This alters the microtubule function and consequently leads to the development of the tauopathy.^[12] The stem-loop structure located at the exon 10-5'-intron junction seems to be an important regulatory element in pre-mRNA splicing. Both in vitro and in vivo experiments have shown that the extent of exon 10 inclusion is inversely proportional to the stability of this structure, a stability that is considerably diminished by mutations (Scheme 1 a).^[13] Thus, small molecules that se-



Scheme 1. a) Sequences and secondary structure of wild-type (wt) and mutated Tau stem-loop target RNAs. Exonic sequences are shown in capital letters and intronic sequences in lower case, with the +3 and +14 FTDP-17 mutations indicated. Nucleotides involved in base pairs identified previously by NMR spectroscopy are connected by a dash.^[13a] When required, biotin or fluorescein derivatization was performed at the 5'-end. The ends of the chains were modified with 2'-O-methylribonucleosides to increase stability with RNases (denoted by an asterisk). b) Structure and peptide sequences of the building blocks used in the DCC experiments.

lectively bind to and stabilize this stem-loop structure, and in particular the mutated variants found in FTDP-17 patients, would allow the physiological balance between Tau isoforms to be restored and, consequently, the disease to be treated.^[14] Importantly, most of the ligands identified in this study by using the DCC approach, in addition to binding with high-to-medium affinity and stabilizing wild-type (wt) RNA, are capable of stabilizing the two mutated sequences (+3 and +14) that cause the highest destabilization of the stem-loop structure.

Results and Discussion

Construction of the dynamic combinatorial library: First, we synthesized several building blocks, including known RNA-binding ligands and some other compounds with the potential to bind to a particular RNA motif, that could be assembled modularly into new lead ligands for Tau stem-loop targets (the structures are shown in Scheme 1 b).^[15] Thiol derivatization was chosen because disulfide exchange is relatively fast in aqueous solutions with pH values near 7–8 and is fully compatible with RNA. In addition, this approach increases the diversity of the dynamic combinatorial library (DCL) in comparison with nonsymmetrical bonds, because the formation of disulfide bridges can afford both homo- and heterodimers.^[16]

Aminoglycoside antibiotics are possibly the most studied RNA ligands. They are known to be able to discriminate A-type from B-type duplexes and to have relatively high affinity for RNA structures.^[2b,17] However, because natural aminoglycosides do not exhibit inherent specificity for biological RNA sequences, several groups have synthesized aminoglycoside analogues to tune specificity without compromising affinity. In order to reduce the risk of nonspecific electrostatic interactions, we decided to select a neamine derivative, Nea, as a building block. This small aminoglycoside incorporates rings I and II of neomycin B and still presents a high charge density. In addition, two acridine derivatives (Acr1 and Acr2) that have the ability either to intercalate in duplex regions or to stack with unpaired nucleobases were also included in the library of monomers.^[18] Although acridines are also promiscuous molecules, they have recently been used in

the development of RNA ligands with high binding affinity and good specificity.^[19] We also selected a third heteroaromatic compound, an azaquinolone derivative, Azq, which could recognize the bulged adenine of the Tau stem-loop and provide higher specificity than the aminoglycosides or intercalators through the formation of complementary hydrogen-bond acceptor–donors.^[20] Finally, two cationic tripeptides containing an aromatic residue, TyrP and TrpP, were assembled by using solid-phase procedures and were included in the library of monomers.

Selection of ligands by using dynamic combinatorial chemistry: In order to facilitate the identification of RNA-interacting molecules, DCC experiments were carried out in a solution phase in the presence of the biotinylated RNA target

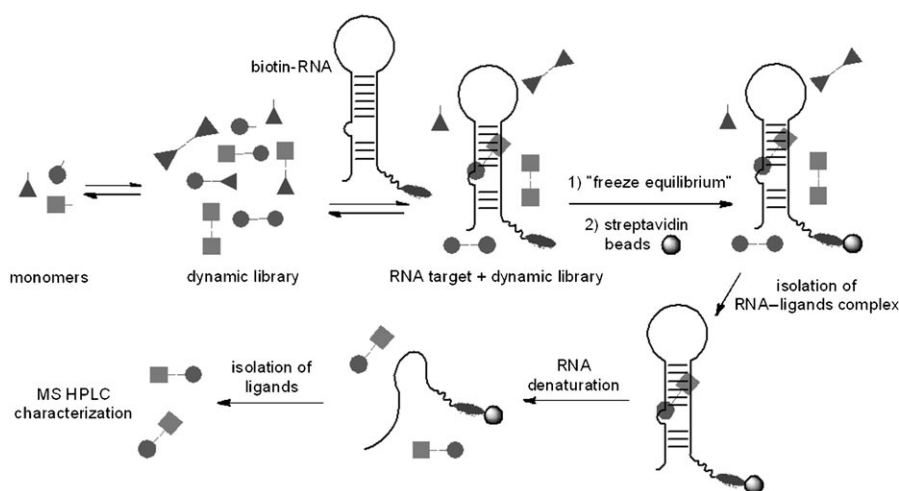


Figure 1. Schematic representation of a DCC process.

(Figure 1). Previously, UV-monitored thermal-denaturation experiments and circular dichroism (CD) spectroscopy had shown that the 5'-end biotin derivatization affects neither the overall stem-loop structure nor its stability (see the Supporting Information). In addition, the unique monophasic curve obtained at a higher concentration (25 μM) was further evidence for the presence of a single intramolecular species (no transitions were detected at low temperatures) and the claim that no supramolecular aggregates are formed during the DCC experiments. After incubation of the thiol-derivatized monomers and the target, the use of streptavidin anchored to magnetic beads allowed the RNA and the interacting ligands to be separated easily from the other members of the DCL.^[7] After denaturation of RNA at 90°C to release any bound ligands, MS-HPLC was used to identify and quantify the compounds. In all cases, a control experiment in the absence of the biotinylated RNA was performed in parallel to determine the effect of the target on the amplification of the ligands.

The first DCC experiment was performed with wt RNA (25 μM) and the Nea, Acr1, Azq, and TyrP monomers (100 μM each) in 50 mM tris(hydroxymethyl)aminomethane-HCl (Tris-HCl) buffer (pH 7.7) containing 100 mM NaCl and 0.1 mM ethylenediaminetetraacetate (EDTA) at room temperature, under an air atmosphere and without stirring. Comparison with the control experiment (in the absence of the RNA) indicated clear amplification of two disulfide heterodimers, Acr1-Nea ($\approx 100\%$) and Azq-Nea ($\approx 75\%$).^[21] Equilibrium was reached within 48 h in both cases, and the composition of the mixture remained unchanged over the next 2 days (see the Supporting Information).^[22] Furthermore, when the Acr1 monomer was replaced by its disulfide dimer, Acr1-Acr1 (50 μM), a similar distribution of products was produced, both in the presence and in the absence of the RNA. This demonstrated that a true thermodynamic equilibrium had been reached and that the air-mediated oxidation process is sufficiently slow to allow for equilibration of the different species.

In subsequent DCC experiments, we included two additional monomers, Acr2 and TrpP, both to increase the diversity of the DCL (21 theoretical compounds may be formed) and to study the competition between the two acridines and the two peptides. As shown in Figure 2, small amplifications of Acr1-Nea (60%) and Azq-Nea (40%) were again observed. However, other new ligands were amplified in much higher proportions, namely, Acr2-Nea (3600%), Acr2-Acr2 (2300%) and, to a lesser extent, TyrP-Acr2 (140%), TrpP-Acr2 (190%), and Azq-Acr2

(200%).^[23] This result indicates that ligands incorporating the Acr2 moiety have a higher affinity for the target RNA than those containing Acr1 or Azq. Importantly, the same species were amplified when the DCC experiment was carried out in the presence of the biotinylated +3-mutated sequence instead of wt RNA (see the Supporting Information). This suggests that the binding site is not close to the mismatched base pair in the +3-mutated sequence.

A crucial parameter in our fragment-based approach is the selection of the appropriate distance between the building blocks to allow the simultaneous recognition of two or more structural motifs in a particular target RNA. This parameter may be used to tune both the binding affinity and specificity of the ligand, as found by Tor and co-workers in some neomycin-acridine conjugates.^[24] With this in mind, we decided to carry out a new DCC experiment with five monomers: Acr2, TyrP, Azq, Nea, and a neamine derivative with a shorter spacer between the aminoglycoside core and the thiol group, Nea2 (Scheme 1b). As expected, the Azq-Nea, Acr2-Nea, and Acr2-Acr2 ligands were amplified in a relative ratio similar to that obtained in the previous experiments (see the Supporting Information). Interestingly, the amplification of the neamine-acridine ligand containing the shorter linker, Acr2-Nea2, was slightly higher than that of Acr2-Nea, which suggests a higher affinity.

Binding affinities and specificities of the selected ligands: In most cases, the selected dimeric ligands were synthesized on a larger scale by replacing the disulfide linkage with a non-reversible thioether isostere ($\text{CH}_2\text{-S}$). Quantitative binding studies were then carried out to determine the binding affinities. Titration experiments were performed by monitoring the quenching of the fluorescence intensity of fluorescein-labeled wt RNA as a function of the increase in the concentration of ligand.^[25] In all cases, a characteristic dose-dependent saturable change in fluorescence was observed, which can be attributed to a slight conformational change in the RNA target induced by the ligand upon complexation (see

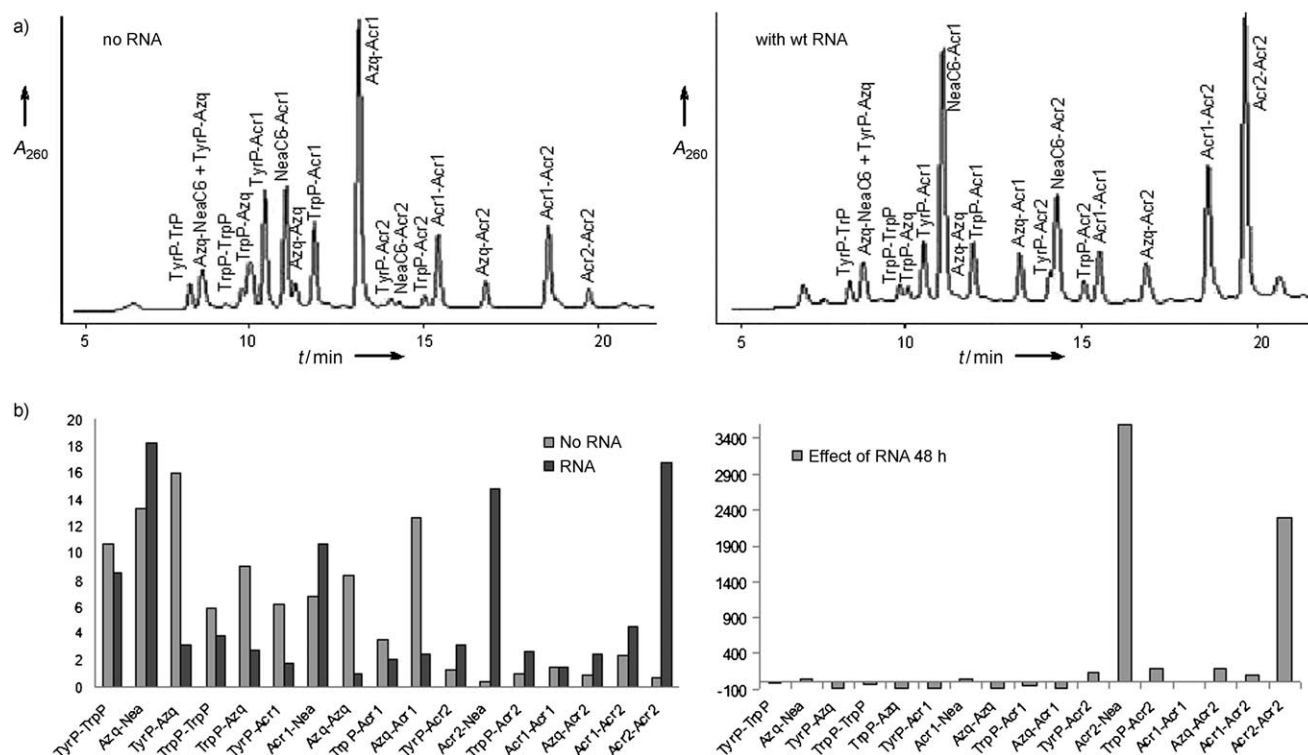


Figure 2. Results of DCC experiments involving wt RNA and the Nea, Acr1, Acr2, Azq, TyrP, and TrpP monomers. a) HPLC traces showing the composition of the DCL in the absence (left) and presence (right) of wt RNA, after 48 h. b) Histograms showing the changes in the DCL composition (left) and the percentage changes (% amplification) of each species (right) upon introduction of the wt RNA.

the CD results below). EC_{50} values (the effective ligand concentration required for 50% RNA response) of 28.6 μM and 58 μM were obtained for Acr1-Nea and Azq-Nea, respectively, by fitting the data in a dose-response curve. As shown in Table 1, the overall results are consistent with the DCC am-

Table 1. Binding of the ligands to wt RNA in the absence or presence of a tRNA competitor.

Ligand	EC_{50} [μM] ^[a]	EC_{50} + tRNA [μM] ^[b]	EC_{50} + tRNA/ EC_{50}
neamine	3300	n.d.	n.d.
Azq-Nea	58.0	n.d.	n.d.
Acr1-Nea	28.6	112.2	3.9
Acr2-Nea	5.9	63.1	10.7
Acr2-Nea2	2.1	47.0	22.4
Acr2-Acr2	2.9	41.0	14.0

[a] All fluorescence measurements (0.25 μM RNA) were performed in 10 mM sodium phosphate buffer (pH 6.8), 100 mM NaCl, and 0.1 mM Na_2EDTA . [b] Measured in the presence of a 30-fold nucleotide excess of a mixture of tRNA (tRNA^{mix}). n.d.: not determined.

plification data because the highest binding affinities are exhibited by the most amplified ligands; this confirms the power of this methodology for identifying ligands for RNA targets. Indeed, ligands containing Acr2 showed higher binding affinities than those containing Azq or Acr1 (EC_{50} = 5.9 and 2.9 μM for Acr2-Nea and Acr2-Acr2, respectively). Interestingly, the binding was observed to be approximately three times stronger for the ligand containing the shorter

spacer between acridine and neamine, Acr2-Nea2, than for Acr2-Nea.

These results prompted us to evaluate the specificity of the ligands. Fluorescence binding assays were repeated in the presence of a 30-fold nucleotide excess of a commercially available tRNA (Table 1), which is a relevant competitor because it contains a mixture of both pre- and mature tRNAs.^[9b,24b,25b,26] Interestingly, the specificity (the EC_{50} value in the presence of the competitor/the EC_{50} value in the absence of the competitor) of the ligands was shown to be highly dependent on the nature of the acridine building block. (The specificity of Azq-Nea could not be determined because the emission maximum of fluorescein varied more than 3 nm at high ligand concentrations.) In the presence of the competitor, the EC_{50} values of Acr2-Nea and Acr2-Acr2 for wt RNA were increased by 11-fold and 14-fold, respectively, whereas that of Acr1-Nea was only increased by 4-fold. Hence, replacement of the Acr2 moiety by Acr1 in the acridine–neamine ligands increases the specificity. On the other hand, as shown in Table 1, the specificity ratio for Acr2-Nea2 was the highest. This result indicates that a longer spacer confers higher specificity in the Acr2–neamine ligands. This trend is different from that previously reported for some acridine–neomycin conjugates with another target, the HIV-1 RRE RNA.^[24b]

These experiments with Tau RNA provide three important conclusions, some of which have also been previously observed in different RNA targets. First, the covalent at-

tachment of a heteroaromatic moiety, either azaquinolone or acridine, causes a substantial increase in the binding affinity of the aminoglycoside scaffold (see the neamine entry in Table 1). Second, ligands containing Acr2 have higher binding affinities than those containing Acr1 and Azq, and it seems that a shorter spacer is preferred in the acridine–neamine ligands with Tau RNA. Third, there is an inverse correlation between affinity and specificity, because the higher the affinity, the less specific the ligand seems to be.

Effect of the selected ligands on the thermal stability of Tau RNA targets:

As previously stated, besides binding with good affinity and specificity to the Tau RNA targets, effective ligands for these targets must stabilize them, in particular the mutated sequences. So, our next objective was to evaluate the ability, if any, of the most amplified ligands to produce stability. The impact of the ligands on the thermal stability of the stem-loop structures (wt and mutated) was estimated by UV-monitored melting experiments (Table 2).

Table 2. Melting temperature (T_m) values for the complexation of ligands with target RNAs (1 μ M of both the RNA and the ligands in 10 mM sodium phosphate buffer (pH 6.8), 100 mM NaCl, and 0.1 mM Na₂EDTA).

Ligand	Wild type		+3 Mutation		+14 Mutation	
	T_m [°]	ΔT_m [a]	T_m [°]	ΔT_m [a]	T_m [°]	ΔT_m [a]
no ligand	66.4	–	50.8	–	54.0	–
neamine	67.6	+1.2	51.8	+1.0	54.4	+0.4
Azq-Nea	67.5	+1.1	51.9	+1.1	54.9	+0.9
Acr1-Nea	67.1	+0.7	52.0	+1.2	54.1	+0.1
Acr2-Nea	68.5	+2.1	53.6	+2.8	56.0	+2.0
Acr2-Nea2	68.8	+2.4	56.5	+5.7	57.2	+3.2
Acr1-Acr1	65.4	–1.0	50.6	–0.2	53.8	–0.2
Acr2-Acr2	67.6	+1.2	53.4	+2.6	55.4	+1.4

[a] $\Delta T_m = (T_m \text{ of the RNA in the presence of ligand}) - (T_m \text{ of RNA alone})$.

In the presence of Azq-Nea or Acr1-Nea, a slight increase in the T_m value was observed in all RNAs ($\Delta T_m \approx +1^\circ\text{C}$), with the exception of Acr1-Nea and the +14 mutant, where no significant shift occurred. This small stabilization, similar to that obtained with neamine alone, could suggest that the Azq or Acr1 fragments do not interact with RNA. However, the binding affinities (Table 1) and spectroscopic data (see below) have demonstrated the active participation of the heteroaromatic moiety in the RNA binding. Replacement of Acr1 by Acr2 in the acridine–neamine ligand (Acr2-Nea) caused a greater increase in the T_m values for both the mutated sequences ($\Delta T_m = +2.8$ and $+2^\circ\text{C}$ for the +3 and +14 mutants, respectively) and the wt RNA ($\Delta T_m = +2.1^\circ\text{C}$). To our surprise, the T_m value of the +3 mutant was clearly increased ($\Delta T_m = +5.7^\circ\text{C}$; Table 2) in the presence of the ligand with the shortest spacer, Acr2-Nea2. The effect of this ligand on wt RNA and the +14 mutant was smaller ($\Delta T_m = +2.4$ and 3.2°C , respectively) but still higher than that induced by the ligand with the longest spacer, Acr2-Nea. It is particularly relevant that the degree of stabilization of the +3 mutant with Acr2-Nea2 is higher than that produced by neomycin B alone and of the same order

as that produced by mitoxantrone, a ligand for Tau RNA recently identified in a high-throughput fluorescence binding assay.^[14a, b, 27]

All together, these results show a direct correlation between the T_m value of the RNA–ligand complex, the level of amplification observed in the DCC experiments, and the binding affinities determined by fluorimetry; this is consistent with previous observations in different systems.^[7,8] The most amplified ligands (Acr2-Nea and Acr2-Nea2) have higher binding affinities and produce a higher degree of stabilization than the least amplified ligands (Azq-Nea and Acr1-Nea). No stabilization was observed upon incubation with Acr1-Acr1 because this compound was not templated by the RNA. As expected, a significant increase in the T_m value also occurred with Acr2-Acr2. These results indicate that the 9-(alkylamino)acridine is more stabilizing than that bearing the 9-carboxamide group. Both the positive charge of the former ($pK_a \approx 5$ for Acr1 versus $pK_a \approx 8$ for Acr2) and its ability to establish additional stabilizing interactions may account for this stabilizing effect and the high binding affinity.^[28]

Spectroscopic studies of the complexes formed between Tau RNA and the selected ligands:

With consideration of the fact that all of the best ligands included a heteroaromatic moiety, we wanted to gain some insight into the role of this group upon complexation with RNA. When Acr1-Nea, Acr2-Nea, and Acr2-Nea2 were titrated with increasing amounts of wt RNA, a strong hypochromism was observed in their UV/Vis spectra (30–40% at a 1:1 ratio; Figure 3). In addition, the 423 and 444 nm bands of the free Acr2-Nea and Acr2-Nea2 ligands exhibited a 7 and 9 nm redshift, respectively. This shift to higher wavelengths was smaller for Acr1-Nea (2 nm for the 360 nm band), which is consistent with previously reported results.^[29] Although a similar hypochromism was observed in the case of Azq-Nea, the interference of the RNA absorbance near the azaquinolone band prevented the titration experiment from being completed (see the Supporting Information). Similar bathochromic effects were observed in fluorescence titration experiments, including reduction in the fluorescence intensity of the acridine moieties together with changes in the spectral profiles (see the Supporting Information). These effects are commonly observed when planar heteroaromatic compounds bind to nucleic acids through an intercalative mechanism or, at least, when stacking occurs with base-pair nucleobases.

Finally, we used CD spectroscopy to check whether these ligands might substantially change the overall conformation of the target RNA structures upon binding. This is a key issue for the recognition of the ligand-stabilized stem-loop by the splicing regulatory machinery. Although the +3 and +14 mutations decrease the thermal stability of the stem-loop RNAs, they exhibit CD spectra that are very similar to that of wt RNA. This indicates that the mutations do not produce a significant change in the structure (see the Supporting Information). When CD spectra were registered in the presence of the selected ligands, minimal alterations

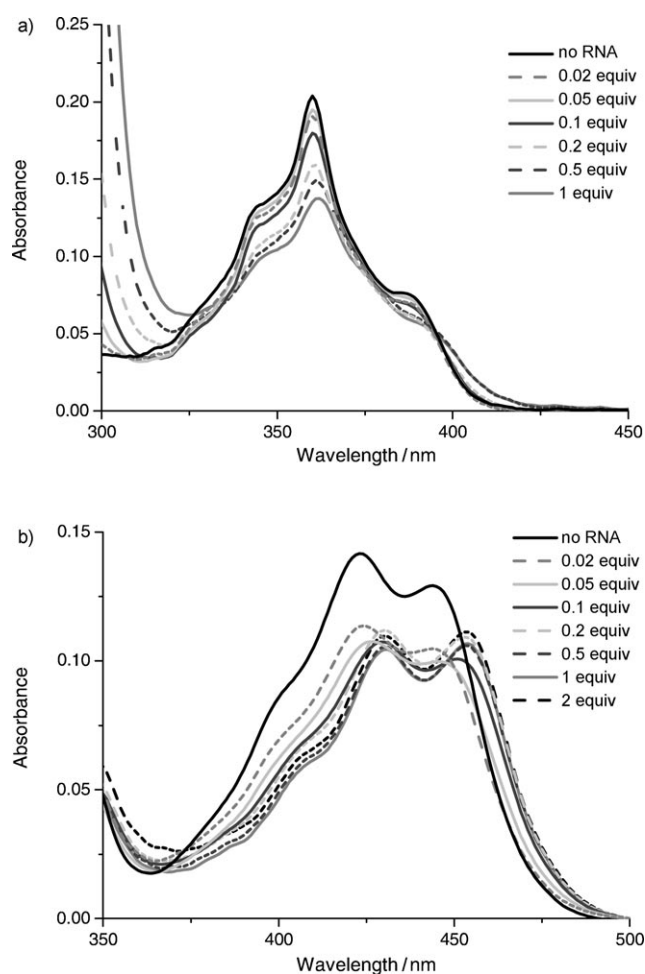


Figure 3. UV/Vis titration of a) Acr1-Nea and b) Acr2-Nea ligands (50 μM) with increasing amounts of wt RNA (0–1 equiv) in a 10 mM sodium phosphate buffer (pH 6.8) containing 100 mM NaCl and 0.1 mM Na_2EDTA .

were observed (a decrease in the ellipticity of the positive band at 234 nm and a concomitant increase in both the intensity and the wavelength shift of the positive band at around 267 nm). These results indicate that the overall stem-loop structure in the Tau RNA target is maintained in all cases. These data, together with the UV/Vis and fluorescence spectroscopy results, suggest that the heteroaromatic moiety of the ligands might intercalate or stack around the bulged adenine, as described by Varani and co-workers for the binding of mitoxantrone to the Tau RNA.^[14c]

Conclusion

In conclusion, we have shown the usefulness of the dynamic combinatorial chemistry approach to identify ligands that bind with high-to-medium affinity ($\text{EC}_{50} = 2\text{--}58 \mu\text{M}$), as determined by fluorimetry, to the Tau exon 10 splicing regulatory element RNA. This confirms the potential of this methodology for developing new RNA-binding compounds. Importantly, most of the selected compounds, which combine a

small aminoglycoside and a heteroaromatic moiety, are able to stabilize the +3 and +14 mutated sequences associated with the development of FTDP-17, as well as the wt RNA. Furthermore, they bind the RNA target without producing a significant change in the overall structure of the stem-loop (as determined by CD spectroscopy), and some of them could have a preferred binding site near the bulged adenine of the stem-loop structure, as suggested by the biophysical experiments. The overall results show a direct correlation between the affinity of the ligands and their stabilizing properties. It is important to point out that the most specific ligands, such as Acr1-Nea, have a moderate affinity for the RNA target, whereas those with high affinities (compounds containing Acr2) are less specific, as inferred from the competition studies performed in the presence of an excess of tRNA.

The identification of ligands that stabilize the mutated Tau stem-loop may open the way for the generation of drugs that restore the physiological balance of Tau isoforms, which may thus allow the treatment of frontotemporal dementias such as FTDP-17, as well as other neurodegenerative tauopathies including Alzheimer's disease. Moreover, these ligands may become valuable tools for studying and understanding the alternative splicing of exon 10 and, for instance, how pre-mRNA secondary structures influence the regulation of alternative splicing.^[12b,30]

Efforts are underway to improve the affinity and especially the specificity of the most promising ligands, as well as to elucidate by NMR spectroscopy the structure of their complexes with both wt RNA and mutated sequences, by using labeled oligoribonucleotides.

Experimental Section

General procedures for DCC experiments: In general, DCC experiments were repeated at least twice in order to confirm their reproducibility. A typical experiment includes the following steps:

A) Quantitation of building blocks and target oligoribonucleotides: In general, building blocks containing thiol were quantified by Ellman's test. Procedure: Ellman's reagent (50 μL ; 2 mM dithio-bis-2-nitrobenzoic acid (DTNB) in 50 mM aqueous NaOAc), aqueous 2M Tris-HCl (100 μL ; pH 8), and H_2O (850 μL minus the sample volume) were added into a 1 cm pathlength quartz cuvette and mixed thoroughly. The UV spectrometer was calibrated to zero at 412 nm. The sample was prepared by adding the appropriate volume (10, 20, 30 μL , etc.) of the thiol. The sample was mixed well and incubated at room temperature for 2 min. The absorbance was measured at 412 nm and the concentration was calculated by using the extinction coefficient ($\epsilon_{412} = 13600 \text{ M}^{-1} \text{ cm}^{-1}$). Although the building blocks were dissolved in 0.1% trifluoroacetic acid (TFA) in H_2O to increase their solubility, the pH value of the Ellman solution was not affected.

For the quantitation of acridine derivatives Acr1 and Acr2, the extinction coefficients of their amino precursors, $\epsilon_{343} = 1979 \text{ M}^{-1} \text{ cm}^{-1}$ and $\epsilon_{361} = 9910 \text{ M}^{-1} \text{ cm}^{-1}$, respectively, were used (determined in 0.1% TFA in H_2O). The concentration of oligoribonucleotides was determined from the 260 nm absorbance value at 25 $^\circ\text{C}$. The extinction coefficient was calculated on the basis of dinucleotide frequencies and composition by using the nearest-neighbor model. The following molar extinction coefficients of ribonucleosides were used for the UV quantitation of oligoribonucleotides: ϵ_i (260 nm): U 9900, A 15400, C 7200, and G 11500 $\text{L mol}^{-1} \text{ cm}^{-1}$.

B) RNA free exchange experiments: Each building block (24 nmol; in 0.1% TFA in H₂O) was combined in an Eppendorf tube and freeze dried or evaporated in a Speed-Vac. Buffer (240 μ L; 50 mM Tris-HCl (pH 7.7), 100 mM NaCl, and 0.1 mM Na₂EDTA) was then added, and the mixture was shaken gently. The DCL mixtures were left to stand at room temperature under air without stirring. After the desired time, an aliquot was taken (approximately one third), the disulfide exchange was stopped by addition of a 0.1% TFA solution in water (100 μ L; pH \approx 2–3), and the mixture was subjected to UV–MS–HPLC analysis.

In some DCC experiments, the building blocks were incorporated as the corresponding disulfide homodimers. In those cases, 12 nmol were used in order to keep the same final concentration of monomer.

C) RNA-templated exchange experiments: Biotinylated RNA (6 nmol; wt or +3-mutated) was annealed in buffer (240 μ L; 50 mM Tris-HCl (pH 7.7), 100 mM NaCl, and 0.1 mM Na₂EDTA) by heating to 90°C for 5 min and then slowly cooling to room temperature. After overnight incubation at room temperature, the solutions were stored at 4°C. The annealed biotinylated RNA was then added to the Eppendorf tube containing the evaporated building blocks, and the resulting mixture left to stand for four days at room temperature under air without stirring. After the desired time, an aliquot was withdrawn (approximately one third), and the disulfide exchange was stopped by addition of 0.1% TFA solution in water (45–70 μ L; pH \approx 5–6).

Streptavidin-coated magnetic beads (Biomag Streptavidin, 5 mg mL⁻¹ suspension, Qiagen) were used to isolate the biotinylated RNA and the binding ligands. In all washing procedures, a magnet was used to retain the beads in the tube while the supernatant was pipetted off. First, the beads (500 μ L of suspension for each DCL aliquot) were separated from the commercial buffer solution and washed with an acidic buffer (3 \times 500 μ L of 50 mM Tris-HCl (pH 5.8), 100 mM NaCl, and 0.1 mM Na₂EDTA). DCL aliquots were added to the washed beads and incubated at room temperature. After 20 min, the beads were retained in the vessel by using the magnet and the supernatant solution was pipetted off again. The beads were then treated to remove the noninteracting ligands and building blocks (3 \times 200 μ L of 50 mM Tris-HCl (pH 5.8), 100 mM NaCl, and 0.1 mM Na₂EDTA). Finally, the beads were washed with a hot solution of 0.1% TFA in H₂O in order to liberate RNA-binding ligands (3 \times 200 μ L, incubation at 90°C for 10 min). The solutions were combined and evaporated in a Speed-Vac. The final residue was dissolved in 0.1% TFA in H₂O and subjected to UV–MS–HPLC analysis.

D) UV–MS–HPLC analysis: UV–MS–HPLC analysis of DCC libraries was performed by using a Micromass ZQ mass spectrometer equipped with an electrospray source and a single quadrupole detector coupled to a Waters 2695 HPLC instrument (photodiode array detector). The detection wavelength was set to 260 nm. Elution was performed on a Grace-Smart C₁₈ column (150 \times 2.1 mm, 5 μ m, flow rate: 0.25 mL min⁻¹) with linear gradients of H₂O and ACN; both solvents contained either 0.1% formic acid or 0.1% formic acid and 0.01% TFA. Typical gradient: 0 to 35% B in 15 min and from 35% to 80% B in 10 min. In some cases, UV–MS–HPLC analysis was carried out with both elution conditions to avoid the overlapping of some peaks in order to allow a more accurate integration.

All peak areas of the HPLC traces were integrated and normalized by taking into account the extinction coefficient of each compound at the detection wavelength: ϵ_{260} : Acr1 37090, Acr2 13334, Azq 2930, TyrP 596, and TrpP 3484 M⁻¹ cm⁻¹. Histograms showing the change in the mol percentage for all DCL members at different times were generated in order to verify that thermodynamic equilibrium had been reached. In addition, histograms showing the mol percentage changes in each species of the equilibrium mixture (amplification%) upon introduction of the target RNA were also generated.

Evaluation of the interaction between RNA and ligands

A) UV-monitored melting experiments: The impact of the ligands on the thermal stability of wt and mutated (+3 and +14) stem-loop RNA structures was estimated by cooling/heating experiments. Samples were placed in 1 cm pathlength quartz cuvettes in a Jasco V-550 spectrophotometer equipped with a thermoregulated cell holder. Melting curves were recorded by cooling the samples from 90 to 20°C at a constant rate of

0.5°C min⁻¹ and measuring the absorbance at 260 nm as a function of temperature. The reverse denaturation curve (20 to 90°C) was then recorded. This cooling/heating experiment ensures that the initial state corresponds to a thermodynamic equilibrium. In all cases, the two curves were superimposable, which indicated that the transition was kinetically reversible. Unless otherwise indicated, the solutions were at a concentration of 1 μ M of both RNA and ligands, in 10 mM sodium phosphate buffer (pH 6.8), 100 mM NaCl, and 0.1 mM Na₂EDTA. The corresponding melting temperature values (T_m) were determined by using the baseline method. All experiments were repeated at least three times until coincident T_m values were obtained. The error in T_m values was \pm 0.2°C.

B) Circular dichroism: Samples were prepared as described in the UV-monitored melting experiment section (3 μ M of both RNA and ligands, in 10 mM sodium phosphate buffer (pH 6.8), 100 mM NaCl, and 0.1 mM Na₂EDTA). Spectra were recorded on a Jasco J-720 spectropolarimeter with a thermoregulated cell holder and interfaced with a Neslab RP-100 water bath, at 20°C. All CD spectra were baseline subtracted with a separately acquired buffer spectrum.

C) UV/Vis titration experiments: A 45–55 μ M solution of the ligand (Acr1-Nea, Acr2-Nea/Nea2, or Azq-Nea) and the corresponding amount of wt RNA (0, 0.02, 0.05, 0.1, 0.2, 0.5, 1, or 2 equivalents) was prepared in 10 mM sodium phosphate buffer (pH 6.8) containing 100 mM NaCl and 0.1 mM Na₂EDTA. The mixture was heated for 5 min to 90°C and left to cool slowly to room temperature. The absorption spectra were recorded at room temperature. The percentage of absorption quenching was determined at the following absorption bands: 360 nm (31%) for Acr1-Nea and 423 (40%) and 444 nm (35%) for Acr2-Nea.

D) Fluorescence titration experiments: A solution of the ligand (Acr1-Nea or Acr2-Nea) and the corresponding amount of wt RNA was prepared in 10 mM sodium phosphate buffer (pH 6.8) containing 100 mM NaCl and 0.1 mM Na₂EDTA. The mixture was heated for 5 min to 90°C and left to cool slowly to room temperature. The fluorescence emission spectra were recorded at room temperature.

E) Fluorescence binding assays: Fluorescence measurements were performed in 1 cm pathlength quartz cells on a QuantaMaster fluorometer (PTI) at 20°C, with an excitation slit width of 4.0 nm and an emission slit width of 5.2 nm. Upon excitation at 490 nm, the emission spectrum was recorded over a range between 500 and 550 nm until no changes in the fluorescence intensity were detected. All binding assays were performed in 10 mM sodium phosphate buffer (pH 6.8), 100 mM NaCl, and 0.1 mM Na₂EDTA.

For each experiment, the fluorescence spectrum of buffer solution (120 μ L) without RNA or ligand was first taken, to be used as the baseline. After this buffer blank, the spectrum of a 0.25 μ M solution of refolded RNA containing fluorescein (120 μ L) was recorded, and the baseline blank was subtracted. Subsequent aliquots of an aqueous ligand solution (1 μ L; increasing in concentration from 0 to 0.75 mM, 0.0005–3000 equivalents, depending on the ligand affinity) were added to the solution containing RNA, and the fluorescence spectrum was recorded after addition of each aliquot until the fluorescein fluorescence signal at 517 nm reached saturation (typically 5–10 min). Over the entire range of ligand concentrations, the emission maxima varied less than 1 nm. The total volume of the sample never changed more than 20%. The full titration was repeated in the absence of labeled RNA to correct for the presence of the ligand's fluorescence. These spectra were subtracted from each corresponding point of the labeled RNA titrations, and the resulting fluorescence intensity was corrected for dilution ($F \times V/V_0$).

The emission fluorescence at 517 nm was normalized by dividing the difference between the observed fluorescence, F , and the initial fluorescence, F_0 , by the difference between the final fluorescence, F_f , and the initial fluorescence, F_0 . This normalized fluorescence intensity was plotted as a function of the logarithm of the total ligand concentration. Finally, nonlinear regression with a sigmoidal dose-response curve was performed with the software package GraphPad Prism 4 (GraphPad Software, San Diego, CA) to calculate the EC₅₀ values. Experimental errors were less than or equal to \pm 25% of each value.

For competitive experiments, a tRNA from baker's yeast (*Saccharomyces cerevisiae*) was purchased from Sigma. Stock solutions of tRNA^{mix} were

quantified by using an average extinction coefficient of 9640 cm^{-1} per base.^[24b] The fluorescence binding assays were carried out as described above with the exception that a 30-fold excess (base) of the tRNA^{mix} was added to the refolded fluorescein-labeled RNA (or to the buffer for the titration without target RNA).

Acknowledgements

The authors wish to thank Prof. Carlos González for fruitful discussions. This work was supported by funds from the Spanish Ministerio de Educación y Ciencia (grant no. CTQ 2007-68014-01/02), the Generalitat de Catalunya (grant no. 2005SGR-693 and the Xarxa de Referència de Biotecnologia), and the Programa d'Intensificació de la Recerca (Universitat de Barcelona). P.L.-S. received a fellowship from the Ministerio de Educación y Ciencia.

- [1] a) J. R. Thomas, P. J. Hergenrother, *Chem. Rev.* **2008**, *108*, 1171–1224; b) F. Aboul-ela, *Future Med. Chem.* **2010**, *2*, 93–119.
- [2] a) J. Gallego, G. Varani, *Acc. Chem. Res.* **2001**, *34*, 836–843; b) Y. Tor, *ChemBioChem* **2003**, *4*, 998–1007; c) N. Foloppe, N. Matassova, F. Aboul-ela, *Drug Discovery Today* **2006**, *11*, 1019–1027; d) T. Hermann, *Biopolymers* **2003**, *70*, 4–18.
- [3] B. Carlson, O. M. Stephens, P. A. Beal, *Biopolymers* **2003**, *70*, 86–102.
- [4] a) S. B. Shuker, P. J. Hajduk, R. P. Meadows, S. W. Fesik, *Science* **1996**, *274*, 1531–1534; b) M. Congreve, G. Chessari, D. Tisi, A. J. Woodhead, *J. Med. Chem.* **2008**, *51*, 3661–3680; c) M. M. Lee, J. L. Childs-Disney, A. Pushechnikov, J. M. French, K. Sobczak, C. A. Thornton, M. D. Disney, *J. Am. Chem. Soc.* **2009**, *131*, 17464–17472.
- [5] a) J. Lehn, A. V. Eliseev, *Science* **2001**, *291*, 2331–2332; b) P. T. Corbett, J. Leclaire, L. Vial, K. R. West, J.-L. Wietor, J. K. M. Sanders, S. Otto, *Chem. Rev.* **2006**, *106*, 3652–3711; c) *Dynamic Combinatorial Chemistry in Drug Discovery, Bioorganic Chemistry, and Materials Science* (Ed.: B. Miller), Wiley, New York, **2010**.
- [6] C. Karan, B. L. Miller, *J. Am. Chem. Soc.* **2001**, *123*, 7455–7456.
- [7] a) A. M. Whitney, S. Ladame, S. Balasubramanian, *Angew. Chem.* **2004**, *116*, 1163–1166; *Angew. Chem. Int. Ed.* **2004**, *43*, 1143–1146; b) S. Ladame, A. M. Whitney, S. Balasubramanian, *Angew. Chem.* **2005**, *117*, 5882–5885; *Angew. Chem. Int. Ed.* **2005**, *44*, 5736–5739; c) A. Bugaut, K. Jantos, J.-L. Wietor, R. Rodriguez, J. K. M. Sanders, S. Balasubramanian, *Angew. Chem.* **2008**, *120*, 2717–2720; *Angew. Chem. Int. Ed.* **2008**, *47*, 2677–2680.
- [8] a) A. Bugaut, J.-J. Toulme, B. Rayner, *Angew. Chem.* **2004**, *116*, 3206–3209; *Angew. Chem. Int. Ed.* **2004**, *43*, 3144–3147; b) A. Bugaut, J.-J. Toulme, B. Rayner, *Org. Biomol. Chem.* **2006**, *4*, 4082–4088.
- [9] a) B. R. McNaughton, P. C. Gareiss, B. L. Miller, *J. Am. Chem. Soc.* **2007**, *129*, 11306–11307; b) P. C. Gareiss, K. Sobczak, B. R. McNaughton, P. B. Palde, C. A. Thornton, B. L. Miller, *J. Am. Chem. Soc.* **2008**, *130*, 16254–16261.
- [10] a) M. Goedert, R. Jakes, *Biochim. Biophys. Acta Mol. Basis Dis.* **2005**, *1739*, 240–250; b) C. Ballatore, V. M.-Y. Lee, J. Q. Trojanowski, *Nat. Rev. Neurosci.* **2007**, *8*, 663–672.
- [11] F. Liu, G. Cheng-Xin, *Mol. Neurodegener.* **2008**, *3*, 8.
- [12] a) K. R. Brunden, J. Q. Trojanowski, V. M.-Y. Lee, *J. Alzheimer's Dis.* **2008**, *14*, 393–399; b) M. S. Wolfe, *J. Biol. Chem.* **2009**, *284*, 6021–6025.
- [13] a) L. Varani, M. Hasegawa, M. G. Spillantini, M. J. Smith, J. R. Murrell, B. Ghetti, A. Klug, M. Goedert, G. Varani, *Proc. Natl. Acad. Sci. USA* **1999**, *96*, 8229–8234; b) C. P. Donahue, C. Muratore, J. Y. Wu, K. S. Kosik, M. S. Wolfe, *J. Biol. Chem.* **2006**, *281*, 23302–23306.
- [14] a) L. Varani, M. G. Spillantini, M. Goedert, G. Varani, *Nucleic Acids Res.* **2000**, *28*, 710–719; b) C. P. Donahue, J. Ni, E. Rozners, M. A. Glicksman, M. S. Wolfe, *J. Biomol. Screening* **2007**, *12*, 789–799; c) S. Zheng, Y. Chen, C. P. Donahue, M. S. Wolfe, G. Varani, *Chem. Biol.* **2009**, *16*, 557–566; d) Y. Liu, E. Peacey, J. Dickson, C. P. Donahue, S. Zheng, G. Varani, M. S. Wolfe, *J. Med. Chem.* **2009**, *52*, 6523–6526.
- [15] Experimental details are provided in the Supporting Information.
- [16] S. Otto, R. L. E. Furlan, J. K. M. Sanders, *Drug Discovery Today* **2002**, *7*, 117–125.
- [17] a) D. P. Arya, L. Xue, B. Willis, *J. Am. Chem. Soc.* **2003**, *125*, 10148–10149; b) K. F. Blount, F. Zhao, T. Hermann, Y. Tor, *J. Am. Chem. Soc.* **2005**, *127*, 9818–9829.
- [18] R. Martínez, L. Chacón-García, *Curr. Med. Chem.* **2005**, *12*, 127–151.
- [19] a) J. F. Arambula, S. R. Ramisetty, A. M. Baranger, S. C. Zimmerman, *Proc. Natl. Acad. Sci. USA* **2009**, *106*, 16068–16073; b) Z. Yan, S. Sikri, D. L. Beveridge, A. M. Baranger, *J. Med. Chem.* **2007**, *50*, 4096–4104.
- [20] S. Hagihara, H. Kumasawa, Y. Goto, G. Hayashi, A. Kobori, I. Saito, K. Nakatani, *Nucleic Acids Res.* **2004**, *32*, 278–286.
- [21] Control experiments showed that the streptavidin-coated magnetic beads did not significantly bind to any of the members of the library or to the ligands; thereby, it was confirmed that amplification of Acr1-Nea and Azq-Nea was a consequence of the RNA templating.
- [22] Although the disulfide-mediated linkage of the four thiol-derivatized monomers may produce up to 10 theoretical dimers, the abundance of only seven compounds was determined. The fact that Nea-Nea, Nea-TyrP, and TyrP-TyrP were eluted very quickly under the conditions used for the HPLC analysis prevented accurate quantification. However, it is noteworthy that close inspection of the MS traces in the presence of RNA revealed a small amplification of Nea-Nea and Nea-TyrP.
- [23] Control experiments in the presence of 0.01% Triton X-100 indicated that the amplification of Acr2-Acr2 and Acr2-Azq was not a consequence of self-recognition of the heteroaromatic moieties (S. L. McGovern, B. T. Helfand, B. Feng, B. K. Shoichet, *J. Med. Chem.* **2003**, *46*, 4265–4272).
- [24] a) S. R. Kirk, N. W. Luedtke, Y. Tor, *J. Am. Chem. Soc.* **2000**, *122*, 980–981; b) N. W. Luedtke, Q. Liu, Y. Tor, *Biochemistry* **2003**, *42*, 11391–11403.
- [25] a) B. Llano-Sotelo, C. S. Chow, *Bioorg. Med. Chem. Lett.* **1999**, *9*, 213–216; b) J. R. Thomas, X. Liu, P. J. Hergenrother, *Biochemistry* **2006**, *45*, 10928–10938.
- [26] S. J. Lee, S. Hyun, J. S. Kieft, J. Yu, *J. Am. Chem. Soc.* **2009**, *131*, 2224–2230.
- [27] Effect of neomycin B (1 equiv): $\Delta T_m = +3^\circ\text{C}$ (wt) and $+5^\circ\text{C}$ (+3 and +14 mutants). It is worth noting that, under our experimental conditions, these values are slightly lower than those previously reported in the literature with the same amount of neomycin.^[14a] Effect of mitoxantrone (1 equiv): $\Delta T_m = +1.9^\circ\text{C}$ (wt), $+6.1^\circ\text{C}$ (+3 mutant), and $+4.8^\circ\text{C}$ (+14 mutant).
- [28] a) S. E. Kitchen, Y.-H. Wang, A. L. Baumstark, W. D. Wilson, D. W. Boykin, *J. Med. Chem.* **1985**, *28*, 940–944; b) F. Hamy, V. Brondani, A. Florsheimer, W. Stark, M. J. Blommers, T. Klimkait, *Biochemistry* **1998**, *37*, 5086–5095.
- [29] S. Sánchez-Carrasco, J. G. Delcros, A. A. Moya-García, F. Sánchez-Jiménez, F. J. Ramírez, *Biophys. Chem.* **2008**, *133*, 54–65.
- [30] a) E. Buratti, F. E. Baralle, *Mol. Cell. Biol.* **2004**, *24*, 10505–10514; b) M. B. Warf, J. A. Berglund, *Trends Biochem. Sci.* **2010**, *35*, 169–178.

Received: July 20, 2010
Published online: January 5, 2011